Published in final edited form as:
J Neural Eng. 2011 June ; 8(3): 036022. doi:10.1088/1741-2560/8/3/036022.

The sodium channel band shapes the response to electric stimulation in retinal ganglion cells

J Jeng[1,2], **S Tang**[3,4], **A Molnar**[4], **N J Desai**[1,2], and **S I Fried**[1,2]

[1]Center for Innovative Visual Rehabilitation, Boston VA Healthcare System, 150 South Huntington Ave, Boston, MA 02130

[2]Department of Neurosurgery, Massachusetts General Hospital and Harvard Medical School, 185 Cambridge Street (3600), Boston, MA 02114

[3]Dept of Natural Sciences, 349 Collins Dr. #7, University of California, Merced, CA 95348

[4]School of Electrical and Computer Engineering, Cornell University, Ithaca, NY 14853

Abstract

To improve the quality of prosthetic vision, it is desirable to understand how targeted retinal neurons respond to stimulation. Unfortunately, the factors that shape the response of a single neuron to stimulation are not well understood. A dense band of voltage gated sodium channels within the proximal axon of retinal ganglion cells is the site most sensitive to electric stimulation, suggesting that band properties are likely to influence the response to stimulation. Here, we examined how three band properties influence sensitivity using a morphologically realistic ganglion cell model in NEURON. Longer bands were more sensitive to short-duration pulses than shorter bands and increasing the distance between band and soma also increased sensitivity. Simulations using the known limits of band length and location resulted in a sensitivity difference of approximately two. Additional simulations tested how changes to sodium channel conductance within the band influenced threshold and found that the sensitivity difference increased to a factor of nearly three. This is close to the factor of 5 difference measured in physiological studies suggesting that band properties contribute significantly to the sensitivity differences found between different types of retinal neurons.

1. Introduction

Retinal degenerative diseases such as macular degeneration and retinitis pigmentosa are the leading cause of blindness in Western countries. These diseases target the outer retina, mainly photoreceptors (the first neuron in the visual pathway), but are thought to leave large populations of inner retinal neurons intact[1–5] (but see also [6]). Electric stimulation of these surviving neurons in blind subjects typically results in light percepts [7; 8]. This raises the possibility that electronic retinal prostheses may be able to restore meaningful levels of vision to the blind. Unfortunately however, the quality and consistency of such percepts is still highly variable[8–10] and therefore, further improvements are needed before these devices can be implemented.

Existing stimulation methods are thought to elicit neural activity that is non-physiological, e.g. quite different from the normal patterns of retinal signaling, and therefore difficult for the brain to interpret. This suggests that better stimulation methods will lead to higher quality percepts. In order to elicit percepts with accurate spatial detail, it is necessary that only those neurons that are close to a given stimulating electrode get activated. However, the structural architecture of the retina imposes challenges to selective activation since axons from ganglion cells traverse the innermost surface of the retina, directly between the

targeted somatic regions of ganglion cells and the stimulating electrodes. Because axons are also sensitive to electric stimulation, the possibility exists that in addition to those ganglion cells that are close to the stimulating electrode, the axons (of distant ganglion cells) that pass close to the same stimulating electrode will also be activated. In-vitro testing supports this notion: the threshold for activation of the passing axons of brisk transient (BT) ganglion cells is only slightly higher (1.8×) than the threshold for activation of the somatic region[11]. If passing axons are activated, the neural signal leaving the retina would appear to arise from a much wider spatial extent than desired and would likely reduce the spatial quality of elicited percepts. A recent study suggests that sub-retinal stimulation can also directly activate ganglion cells (and/or perhaps their axons)[12], raising concerns about spatial quality for both locations of the stimulating electrode.

To develop stimulation methods that activate the somatic region without simultaneously activating passing axons, it is desirable to understand the mechanism by which each of these elements becomes excited. The mechanism by which axons are activated has been studied extensively and is well understood for a wide range of stimulation parameters and axonal properties. In contrast, the mechanism(s) by which the somatic region is activated by electric stimulation is not well understood and therefore, it is important to gain insight into this process as a step towards developing more effective stimulation methods.

Several previous computational studies explored the response of the somatic region to stimulation in modeled ganglion cells[13; 14]. In each study thresholds for activation were lowest in the soma or initial segment (proximal axon) but the specific neuronal element found to have the lowest threshold was different in each study. In addition, none of the previous models included a dense band of sodium channels known to exist within the proximal axon. This band was recently shown to have the highest sensitivity in response to electric stimulation[15] suggesting that it plays a key role in the activation process. Interestingly, the length and location of the band is different in different sub-types of retinal ganglion cells. This raises the possibility that differences in band properties could underlie the different sensitivities to electric stimulation known to exist across retinal ganglion cell sub-types[15; 16].

In this study, we simulated the response of a morphologically-realistic retinal ganglion cell model to electric stimulation with the NEURON simulation program[17]. The modeled cell included a dense region of voltage gated sodium channels in the proximal axon. The properties of the sodium channel band were adjusted over the ranges known to exist from anatomical and physiological studies. Consistent with previous physiological results, we found that the sodium channel band is the site of lowest threshold. Also, we found that the band is the site in which spikes are initiated although the spike initiation site was sensitive to the location of the stimulating electrode as well as to the amplitude of the stimulus (relative to threshold). In addition, we found that the sodium channel density within the band as well as the length and location of the band all had a significant effect on the cell's sensitivity to electric stimulation. The implications of these findings for developing more effective stimulation strategies are discussed.

2. Methods

2.1. Cell properties

We used NEURON[17] to study the response of modeled retinal ganglion cells to electric stimulation. The multi-compartment ganglion cells used in this study were based on a previously developed cell model that was traced from an actual tiger salamander ganglion cell [18] – the compartments representing the dendrites and soma of the modeled cells in the present study were identical to those of the previous model and did not vary. The soma

consisted of stacked cylinders, the central axis of each was parallel to the central axis of the axon. An axon with four different regions (each with multiple compartments) was added to the soma/dendrite compartments – the regions are depicted schematically in Figure 2a. The axon hillock (AH) and sodium channel band (SOCB) regions each had variable properties, allowing us to study how band properties influenced the response to electric stimulation. The ion channel conductances associated with each region are listed in Table 1. The axon hillock (AH) region refers to the portion of the axon that emerges from the soma. The AH was connected to the right-most edge of the horizontal midline of the soma (left/right and up/down descriptions refer to the orientation of the model cell in Fig. 2a) and extended 0.5 μm horizontally. The first bend of the AH was defined by an angle that extended 15 μm down and 4.5 μm to the right. The second bend of the axon fixed the trajectory of the axon so that its height remained 15 μm below and parallel to the midline of the soma. At this height, the axon was 5 μm below the bottom edge of the soma.

The sodium channel band (SOCB) region is the portion of the axon attached and immediately distal to the AH. Anatomical parameters were adapted from Fried et al [15] unless specified. The diameter within the SOCB tapered from 3.0 μm at its proximal end to 0.8 μm at the distal end (proximal and distal refer to the directions towards and away from the soma, respectively). To determine the effect of band properties on the ganglion cell's responsiveness to electric stimulation, the length of the band as well as the channel conductances within the band were both modified as described in the text. In addition, the length of the portion of the AH distal to the second bend was adjusted in order to move the band closer to or further from the soma. The thin section (TS) region of the axon was immediately distal to the SOCB; its properties were derived from the work of Carras et al[19] and remained fixed throughout this study. Distal to the TS was the distal axon (DA) region (not shown in Fig. 2a); properties remained constant within this region as well. The number of compartments comprising each region is given in Table 1.

2.2. Cell membrane model

Similar to previous modeling studies that have explored the response of retinal ganglion cells to electric stimulation[13; 14; 20; 21], we used five active membrane currents plus a leak current to simulate the cell membrane. These include the voltage-gated sodium current I_{Na}, the delayed rectifier non-inactivating potassium current I_{DR}, the inactivating A-type potassium current I_A, the calcium-activated potassium current (non-inactivating) $I_{K,Ca}$ and a calcium current I_{Ca}. The $I_{K,Ca}$ current was activated by the level of intracellular calcium; all other active channels were modeled as voltage-gated. Kirchoff's law yields the equation for membrane potential:

$$C_m dE/dt = -\widehat{G}_{Na} m^3 h(E-E_{Na}) - \widehat{G}_{Ca} c^3 (E-E_{Ca}) - \widehat{G}_{K,DR} n^4 (E-E_K) - \widehat{G}_A a^3 h_A (E-E_K) - \widehat{G}_{K,Ca} (E-E_K) - \widehat{G}_l (E-E_l) \quad (1)$$

where E_{Na} = +35mV, E_K = −75mV, E_{Ca} = + 132.46 mV and E_l = −65 mV. Values for $\hat{G}_{Na}$, $\hat{G}_{Ca}$ $\hat{G}_{K,DR}$, $\hat{G}_A$ and $\hat{G}_l$ varied across different regions of the modeled cell and are given in Table 1. The rate constants: m, h, c, n, a and h_A are all determined by the equation:

$$dx/dt = -(\alpha_x + \beta_x) \bullet x + \alpha_x \quad (2)$$

where both α and β are functions of voltage (Table 2).

Conductances in Table 1 were adapted from Sheasby and Fohlmeister[18] unless specified; empty boxes indicate zero conductance in that region. The variation in $\hat{G}_{Na}$ was tested in one of the experiments; rationale for the range is described in detail (see Results). Increases in

$\hat{G}_{Na}$ sometimes caused spontaneous spikes to occur; these were eliminated with corresponding increases in $\hat{G}_{K,DR}$. Membrane capacitance, C_m, was fixed at 1 μF/cm^2.

2.3. Electric stimulation

The stimulating electrode was modeled as an ideal monopolar point source of current. The external medium was assumed to be homogeneous, of infinite extent and linear. The height of the stimulating electrode was fixed at 25 μm from the axon (Fig. 2b); this height was identical to that used in previous physiological studies to allow for direct comparison of results. In most model experiments, the position of the stimulating electrode was stepped in 2 μm increments along a line parallel to the long axis of the axon and the threshold for activation determined at each location. The duration of the rectangular stimulus pulse was fixed at 200 μsec. The electric field was derived from the equation

$$V_e=(\rho_e I)/(4\pi r) \tag{3}$$

where V_e = the extracellular potential, I = the amplitude of the constant current pulse, ρ_e = the resistivity of the retinal extracellular solution (typically Ames medium, set to [110] Ω•cm) and r is the distance between the stimulating electrode and the point at which the voltage is being computed. Non-uniformities in the electric field arising from the presence of the model cell, or other nearby neuronal elements, were not considered.

Simulations involving disk electrodes were adapted from those of Greenberg et al [14]; the electric field for the disk electrode was derived from the equation

$$V(r,z)=\frac{2V_n}{z}sin^{-1}\left(\frac{2a}{\sqrt{[(r-a)^2+z^2]}+\sqrt{[(r+a)^2+z^2]}}\right) \tag{4}$$

where V(r,z) = the extracellular potential, r, z = the respective radial and axial distances from the center of the disk when z≠0, V_0 = the potential on the surface of the disk, and a is the radius of the disk. Subsequently, the method for incorporating these extracellular potentials into the NEURON model was identical to that of the point source electrode. The electrode position of each disk electrode was defined by the center of the disk.

For each simulation the extracellular voltage was computed for a point at the center of each cylindrical compartment and applied uniformly to the extracellular surface of the entire compartment. This voltage was incorporated into the NEURON simulation environment and the resulting V_m of each compartment was calculated. The threshold for eliciting a propagating action potential was calculated to within 0.1 μA.

3. Results

In physiological experiments with retinal ganglion cells and a small stimulating electrode, the lowest activation thresholds occurred when the electrode was positioned over the proximal axon, approximately 40 μm from the ganglion cell soma[15] (Fig. 1a). Overlay of the ‘threshold map’ with the dye-filled ganglion cell revealed that the low threshold region corresponds to the proximal axon (Fig. 1b). Immunostaining for AnkyrinG, a structural protein associated with dense regions of voltage-gated sodium channels[22; 23], revealed a dense band of staining in the proximal axon that was spatially aligned with the low threshold region (Figs. 1c, d). This suggests that the sodium channel band has the highest sensitivity to electric stimulation and therefore, the properties of the band are likely to modulate the response to electric stimulation.

To explore the role of the band, we developed a multi-compartment morphologically realistic ganglion cell model in NEURON (Fig. 2a, Methods) and simulated the response to stimulation from a small point-source electrode. The model cell was nearly identical to that used in previous studies[18] but was modified to include a dense region of voltage-gated sodium channels (sodium channel band) in the proximal axon (Fig. 2a, red) (Methods). The length and location of the band were varied to approximate the range of values reported in previous studies[15; 24]. The conductance of voltage gated sodium channels within the band ($\hat{G}_{Na}$) is not known and therefore a range of values as suggested by previous studies (discussed below) were evaluated.

A typical simulation, measuring threshold as a function of the stimulating electrode's position along a one dimensional line 25 μm away from and parallel to the axon, is shown in Figure 2b. Consistent with previous physiological measurements[15] (e.g., Fig. 1), the lowest thresholds were found when the stimulating electrode was approximately centered over the dense band of sodium channels. The proximal and distal edges of the band were 30 and 70 μm from the soma (respectively). The absolute minimum threshold occurred when the stimulating electrode was 54 μm from the soma – distal from the center of the band by 4 μm. Typically, the point of lowest threshold was offset from the center of the band (away from the soma) although the amount of offset was dependent on the properties of the band (discussed below).

The effectiveness with which a given stimulus activates only those neurons close to the stimulating electrode, e.g. avoids the activation of passing axons, can be estimated by studying the relative thresholds for activation of the somatic region (including the sodium channel band) vs. activation of the distal axon. For example, if the threshold for activating the distal (passing) axon is high relative to the threshold for activating the somatic/band region, only those neurons with sodium channel bands close to the stimulating electrode will be activated. In contrast, a ratio of one suggests that both axons and somatic regions (bands) near the stimulating electrode are equally likely to be activated. Thus, the ratio of thresholds can be used to compare the relative effectiveness between different stimulus configurations. For the simulation in Figure 2, the minimum threshold for activation in the band region was 30 μA while the threshold when the stimulating electrode was over the distal axon was 71 μA. The ratio, 2.34, suggests that neurons close to the stimulating electrode will be preferentially activated vs. passing axons.

3.1. Band properties influence thresholds

The ratio between thresholds (distal axon vs. band) was highly sensitive to changes in band properties (Figs. 3–5). To facilitate comparisons, the properties of the thin segment (TS) and the distal axon (DA) portions of the axon were kept constant in all simulations so that thresholds across these regions did not vary. As a result, changes in the threshold ratio were due solely to changes in threshold of the band/somatic region. We report the ratios (distal axon/band), instead of the absolute threshold levels in the band, because normalization to the distal axon threshold level provides additional relevance.

In previous simulations[13; 14], $\hat{G}_{Na}$ of the distal axon was set between 50 and 100 mS/cm^2 while the maximum conductance ranged from 100 to 150 mS/cm^2 and was typically assigned to the initial segment (proximal portion of the axon). Thus, the ratio of conductance (proximal axon to soma) in previous models ranges from 2 to 3. While there are no direct measurements in the retina that refute these estimates (the actual conductances are not known), the ratios appear low given the patterns of immunochemical staining seen in the band and somatic region[15; 24; 25] (e.g. Fig. 1d). Even though great care must be taken in trying to quantify anatomical differences underlying different levels of fluorescent staining, additional support for a higher ratio comes from direct measurements of sodium channel

conductance in non-retinal neurons[26]. These studies suggest that $\hat{G}_{Na}$ ratio (band/soma) is possibly as high as 50. In our model cell $\hat{G}_{Na}$ of the distal axon was set to 70 mS/cm^2 and $\hat{G}_{Na}$ of the band was varied from 350–2800 mS/cm^2. Thus, the ratio of G_{Na} (band/distal axon) that we tested ranged from 5–40. ($\hat{G}_{Na}$ for the soma and the distal axon were nearly identical so the $\hat{G}_{Na}$ ratios for band/distal axon and band/soma are used interchangeably). The lower limit is comparable to the ratios used in previous studies; the upper limit is comparable to the estimates from non-retinal neurons.

The shape of the one-dimensional threshold maps was generally similar across the range of $\hat{G}_{Na}$ ratios that we tested (Fig. 3). However, the minimum threshold in the band region varied inversely with the $\hat{G}_{Na}$ level: the lowest thresholds were associated with the highest $\hat{G}_{Na}$'s. The resulting distal-axon/band threshold ratios varied from 1.56 when the band/distal axon $\hat{G}_{Na}$ ratio was 5 to 2.82 when the ratio was 40. The lowest threshold always occurred at the same location for a given band length and location, e.g. offset by ~4 μm from center for a band that was 40 μm long when the closest edge was 30 μm from the soma.

The absolute minimum value of threshold in the band region was also found to vary with changes in both the length and location of the band (Fig. 4). Previous studies have identified the range of band length and location across different types of ganglion cells[15; 24]. To explore whether the range of values suggested by those studies influenced the response to electric stimulation, we ran the simulations shown in Figure 4. They revealed several important insights about how band length and location influence the response to electric stimulation. First, the simulations indicate that longer bands are associated with lower thresholds (Fig. 4a, b). Second, thresholds decreased as the distance between band and soma increased. This can be seen by comparing a 20 μm band whose left edge is fixed 30 μm from the soma (Fig 4a) to the same length band when the left edge was fixed 50 μm from the soma (Fig. 4b). In general, the decrease in threshold was not uniform as the band was moved further from the soma but depended on both the length and the location of the band. The third insight revealed by the simulations of Figure 4 is that the effects of band length and band location on threshold were dependent on each other. This can best be seen by comparing the reduction in threshold for increasing band lengths in Fig. 4a to the corresponding reductions in Fig. 4b. Neither the magnitude of reduction nor the overall pattern of reduction was similar. For example, when a 60 μm band whose left edge was 10 μm from the soma (Fig. 4b) was moved 20 μm so that the left edge was now 30 μm from the soma (Fig. 4a), the threshold was reduced, but the amount was smaller than the reduction for the 20 μm movement described above. Examination of Figure 4b reveals that the location at which threshold was lowest was nearly identical for all three band lengths and was close to the distal (right) edge of the band. This suggests that the location of the distal edge of the band influences threshold. Band length contributes, but once length exceeds a certain value, it no longer influences threshold. Taken together, these results suggest that long bands whose distal edge is far from the soma will have the lowest thresholds.

To estimate the range of thresholds that might be expected across the population of ganglion cells, we compared the threshold response to a ganglion cell that had a short band with low G_{Na} that was close to the soma (low-threshold model) to a cell that had a long band with high $\hat{G}_{Na}$ that was far from the soma (high-threshold model) (Fig. 5). The minimum thresholds for the low- and high-threshold models were 22.8 and 53.2 μA respectively. These presumed upper and lower limits differ by a factor of ~2.3. Thus, our results suggest that different sub-types of ganglion cells will have different sensitivities to electric stimulation and is consistent with previous physiological studies in which three different types of ganglion cells each had a different threshold in response to 0.1 ms cathodal pulses[15]. The range of thresholds suggested by the simulations in this study is slightly less than those found physiologically (~5), suggesting that other factors, not tested in this study,

also contribute to threshold. The threshold for the distal axon remained fixed at 71 μA; thus the limits of the threshold/band ratio ranged from 1.33 to 3.1. This raises the possibility that the ability to avoid the activation of axons may also vary across different types of ganglion cells (Discussion).

Thus far the waveform used for stimulation has been a monophasic (cathodal) pulse of 0.2 ms. In clinical use however, it will be necessary to apply charge-balanced waveforms in order to prevent damage to both electrode and tissue. We explored the effect of adding an equal and opposite anodal pulse immediately following the cathodal phase (Fig. 6a, left). Interestingly, addition of the anodal phase had little impact on the low-threshold model when the stimulating electrode was positioned over the band region (Fig. 6a, right) but when the electrode was moved further out along the axon, biphasic pulses were associated with higher threshold responses – compare dashed and solid green lines). This resulted in an increase in the axonal to band threshold ratio for biphasic pulses (as compared to monophasic cathodal pulses), i.e. ratios were 3.93 and 3.06 for biphasic and cathodal, respectively. In the low-threshold model, thresholds were higher for biphasic pulses at all locations of the stimulating electrode resulting in a much smaller change in the axonal to band threshold ratio (1.38 vs. 1.35). This suggests that biphasic pulses may be more effective than monophasic pulses in avoiding axons but only for certain types of ganglion cells. The effect may be even stronger for other types of biphasic pulses, i.e. non-symmetric charge-balanced, but these were not tested in this study.

We also tested the effect of changing the stimulating electrode from a point source to a disk electrode (Fig. 6b) (Methods). Diameters of 10, 50 and 200 um were tested (left, middle and right panels, respectively). In general, the pattern of thresholds was similar to that of the point source and the ratio of thresholds (minimum for the high threshold model/minimum for the low threshold model) (2.35, 2.50 and 2.46 respectively) did not vary considerably from the ratio for the point source electrode (2.33). Note that the minimum threshold for the 200 um disk electrode occurred when the stimulating electrode was centered approximately 80 um from the center of the band. This was likely the result of the larger electric fields associated with the periphery of disk electrodes.

3.2. Site of spike initiation is within the sodium channel band

For each set of band parameters, we determined the site of spike initiation in response to multiple locations of the stimulating electrode (the same locations for which the one-dimensional threshold maps were obtained) (Fig. 6). The site of spike initiation was defined as the model compartment whose membrane voltage first crossed 0 mV. A typical response is shown in Figure 6a (distal axon/band $\hat{G}_{Na}$ ratio = 5). Generally, the site of spike initiation followed the position of the stimulating electrode, although, for locations near the band the site of spike initiation was always within the band and generally within the distal half. For higher G_{Na} ratios (Fig. 6b, ratio = 40), the site of spike initiation remained within the band for a wider range of stimulating electrode locations. This can be seen by comparing the site of spike initiation when the stimulating electrode is positioned at 100 μm in Figures 6a and 6b (vertical line). Note that the site of spike initiation could be inferred somewhat from the threshold profile: for stimulating electrode positions associated with thresholds significantly below the threshold of the distal axon, the site of spike initiation tended to be within the band. Once the threshold associated with a given stimulating electrode position approached that of the distal axon, the site of spike initiation shifted towards to the stimulating electrode position.

We also explored whether the site of spike initiation changed as a function of stimulus amplitude (Fig. 6c, d). For lower stimulus amplitudes, e.g. those closest to threshold, the site of spike initiation remained within the band for a wider range of stimulating electrode

locations. At higher stimulus amplitudes, the site of spike initiation more closely followed the position of the stimulating electrode. At these higher stimulus amplitudes however, increasing the G_{Na} ratio resulted in the site of spike initiation remaining within the band for a wider range of stimulating electrode locations.

4. Discussion

Improvements in the quality of prosthetic vision will arise from the development of more sophisticated stimulation schemes, including ones that can selectively activate specific types of ganglion cells and/or selectively avoid passing axons. These schemes will bring the neuronal activity elicited by the prosthetic more in line with the retina's physiological signaling patterns and presumably make the neural signal that reaches the brain easier to interpret. The development of such schemes will be derived from an improved understanding of the neuronal features that shape the response of retinal neurons to electric stimulation. Towards this end, the goal of this study was to explore how the properties of the sodium channel band influence the ganglion cell response to extracellular electric stimulation. Consistent with previous physiological studies, the model confirmed that the band is the neuronal element with the highest sensitivity to electric stimulation. Further, the model predicts that specific properties of the band influence the cell's sensitivity to electric stimulation. Knowledge of the band properties for different ganglion cell types will enable their relative sensitivity to be predicted and therefore, may allow inferences of the neural activity underlying psychophysical percepts to be made.

4.1. Band properties influence the response to electric stimulation

We found that at least three properties of the model band influence the response to electric stimulation. These include the sodium channel conductance within the band, the length of the band and the location of the band relative to the soma. In addition, our results suggest that band length and location do not act independently in shaping the response to electric stimulation.

4.1.1. Influence of sodium channel conductance—The voltage gated sodium channel conductances within the ganglion cell are not known. Previous simulations[13; 27] used conductances of 150 and 50 – 100 mS/cm^2 in the proximal and distal axon respectively and 70 mS/cm^2 in the soma; with these values, the ratio of conductance in the proximal vs. distal axon ranged from 1.5 – 3 and the proximal axon to soma ratio was ~2. Conductances of 70 and 80 mS/cm^2 were used in the current model for the soma and distal axon respectively, making the band conductance similar for both regions. We believe the higher ratios (5–40) that we tested are justified for two reasons. First, the immunochemical staining patterns associated with AnkyrinG (a structural protein associated with dense regions of voltage gated sodium channels), e.g. Fig. 1d, suggest that the density of sodium channels in the band is much higher than the density along the distal axon. This staining pattern was consistent for other immunochemical markers as well including ones that tagged sodium channels directly[15; 24; 25], minimizing the possibility that the staining pattern reflects a difference in something other than the sodium channel distribution. The second reason we tested higher $\hat{G}_{Na}$ ratios in our study derives from previous work that investigated the action potential initiation process in layer 5 pyramidal neurons of rat cortex[26]. These studies used a combination of electrophysiology, immunochemistry, modeling and Na+ imaging to conclude that $\hat{G}_{Na}$ in the band is ~50× that of $\hat{G}_{NaNa}$ in the soma. This high ratio ensures that in response to synaptic input, the action potential is elicited consistently in the band. Many elements of the activation mechanism in retinal ganglion cells[19] are thought to be similar to those in pyramidal cells, including the site of spike initiation. These similarities increase

the likelihood that a comparably high ratio of band/soma conductance exists in retinal ganglion cells.

The level of sodium channel conductance within the band influenced the response to electric stimulation. For example, increasing $\hat{G}_{Na}$ reduced threshold such that each successive doubling of $\hat{G}_{Na}$ in the band reduced threshold by a comparable amount (Fig. 3). Comparing the lowest (5) and highest (40) ratios that we tested in the model yielded thresholds that differed by a factor of 1.8. It is difficult to predict the actual amount by which $\hat{G}_{Na}$ variations will influence physiological thresholds across ganglion cell types. If we assume that the range of the sodium channel conductance ratios remain high in all ganglion cell types, and the range of conductance ratios is within a factor of two (e.g. between 20 and 40), the corresponding thresholds across types will range within ~25% (25 to 31 μA – Table 3). Thus, we can infer that the range of threshold differences arising from variations of band $\hat{G}_{Na}$ will be limited, provided the $\hat{G}_{Na}$ ratio is 'high' in all types.

The estimates of sodium channel conductance that we used suggest three additional limitations of this study. First, recent work indicates that at least two sub-types of voltage gated sodium channels exist within the band[24]. The kinetics of each sub-type is thought to be different[28] raising the possibility that the sensitivity of each sub-type to extracellular electric stimulation may be different as well. If the distribution of each sodium channel sub-type varies across ganglion cell types, such differences could serve to alter the range of thresholds across ganglion cell types that were found here. Second, because increases to the sodium channel conductance in the band sometimes caused spontaneous spikes to occur in the model, we needed to increase the potassium conductance in the band as well (see Methods). Increases in the potassium conductance are associated with increases in threshold (potassium currents have opposing effects to sodium currents) and therefore, it is possible that the actual reductions in threshold associated with increases in sodium conductance are actually slightly larger than what we report here. The actual sodium and potassium conductances within the band are not yet known. Third, , the sodium channel conductances for neuronal elements other than the band were kept uniform in the model while in actuality these conductances vary considerably. In addition, the degree of heterogeneity can differ across different types of ganglion cells. The effect of these differences on the response to stimulation was not explored in this study.

4.1.2. Influence of band length and location—The activation threshold in response to electric stimulation was also modulated by both the length of the band as well as its location relative to the soma. In general, lengthening the band or moving it further from the soma each resulted in a reduction of the activation threshold. Interestingly however, the sensitivity to changes in the two parameters did not operate independently. For example, when the left edge of the band was held fixed, increases in band length reduced threshold (Fig. 4a). In contrast, when the right edge of the band was held fixed (Fig. 4b), increasing the band length reduced threshold in some cases (from 20–40 μm) but not in other cases (from 40–60 μm). The threshold patterns in Figure 4b suggest that the distance of the distal edge of the band from the soma strongly determines the minimum threshold that can be realized – the larger the distance, the lower the threshold. Given that simulations also indicate that spikes were usually initiated close to the distal edge of the band, it is not surprising that it is the location of this edge that most strongly affects threshold. The minimum threshold results only for band lengths above a minimum value (~ 40 μm). If the band length is below that minimum, threshold increases. The decrease in threshold as the band was moved away from the soma (Fig. 4a) was not unexpected given that the high capacitance of the soma will tend to shunt current from more proximal locations during spike initiation.

Comparing threshold at the extremes of length and location (long band that was far from the soma vs. short band close to the soma) yielded values of 0.0283 and 0.0354 mA respectively (factor of 1.25). This suggests that the threshold differences arising from differences in band length/location are comparable in magnitude to those arising from changes in band $\hat{G}_{Na}$. By incorporating the highest $\hat{G}_{Na}$ into the long band that was furthest from the soma and the lowest $\hat{G}_{Na}$ into the shortest band that was closest to the soma, we were able to estimate the range of thresholds that might be expected across the population of ganglion cells (Fig. 5). The thresholds derived from these two models differed by a factor of ~3. This is consistent with a previous physiological study that found that threshold varied by a factor of 5 across three different types of rabbit retinal ganglion cells[15]. Thus, our modeling results are in fairly close agreement with physiological measurements. The wider range of thresholds observed physiologically may arise because additional properties of ganglion cells (not tested in this study), also influence the response to electric stimulation. These include morphological properties such as soma size, axon diameter and the extent of the dendritic field which are known to vary considerably across the different types of ganglion cells[29] as well as the distribution and density of individual ion channels within each type of ganglion cell.

In addition to the absolute threshold differences between types that were described above, our results also suggest that the ratio of threshold between the band and the distal axon is likely to vary for different types of ganglion cells. In our simulations, all properties of the thin segment and the distal axon remained constant and therefore the threshold for stimulation over the distal axon remained constant as well. Under these conditions the range of band/distal axon thresholds that we found was 1.33 to 3.11. This range is consistent with a physiological study in which the ratio was found to be ~1.8 in brisk transient rabbit ganglion cells[11]. Since properties of the distal axon (e.g. diameter, conduction velocity) vary between different types of ganglion cells, it is likely that axonal thresholds will vary across types as well. Although we did not test the effect of varying axonal properties in this study, it is straightforward to hypothesize that variations in threshold along the distal axon will serve to lower the band/distal axon threshold ratio in some types and increase the ratio in others. As a result, the distribution of threshold ratios is likely to be wider than what we describe here. It will be quite difficult to elicit focal activity in ganglion cell types that have ratios close to one (or lower), raising the possibility that the improved quality of spatial percepts reported during recent clinical trials[30; 31] may be the result of focal activation within some but not all types of ganglion cells.

4.1.3. Influence of stimulation parameters—Both the stimulus waveform and electrode size were found to influence the response to stimulation as well. These were tested for only one alternative waveform and only a few disk sizes. Nevertheless, these results suggest that different waveforms and/or electrode configurations can modulate the differences that we found with monophasic (cathodal) pulses from a point source. While the biphasic pulse tested in Figure 6a increased the threshold difference between the band and distal axon regions for the low threshold model cell, it resulted in only a small difference for the high threshold cell. This raises the possibility that other changes to the stimulus waveform may be even more effective for increasing the axonal to band threshold ratio and further testing is warranted. Changes in electrode diameter had only a modest effect on the threshold ratio (Fig. 6b). The location of the stimulating electrode for the largest diameter electrode we evaluated (200 um) was offset from the band, probably because the electric field associated with disk electrodes is highest at the periphery. Thus, the threshold ratio (band/distal axon) is likely to vary for the population of ganglion cells lying underneath a given large-diameter stimulating electrode.

4.2. Applicability to other neural prosthetics

The results we describe here for the retina are likely to apply to a wide range of neural prosthetics that target other regions of the CNS. Sodium channel bands have been identified in neurons from many different regions of the CNS and band differences have been identified for other types of neurons (in addition to retina). Therefore, our findings suggest that different types of neurons within each region of the CNS are likely to have different sensitivities to electric stimulation. If this is the case it is likely that only those types with the lowest thresholds are responding. Knowledge of the sodium channel band properties for each neuron within a given region will improve the ability to predict selectivity. Similar to the retina, it has proven challenging to avoid the activation of axons in many of these other neural prosthetic applications as well. By identifying the factors that influence sensitivity of the band region, our results may lead to improved stimulation methods, e.g. those that can avoid axonal activation.

4.3. The band is the site of spike initiation

For stimulation in and around the band region, we found that spikes were initiated within the band (Fig. 6). While there was some evidence that spikes could be initiated in the soma when the stimulating electrode was very close (to the soma), the site of initiation quickly shifted to the band once the stimulating electrode was moved over the AH portion of the axon. The site of spike initiation remained within the band for stimulating electrode positions as much as 30 μm on either side of the band. The site of spike initiation was highly sensitive to stimulation level (relative to threshold) however, and moved closer to the stimulating electrode as the stimulus level was increased.

Interestingly, the site of lowest threshold did not always align with the site of spike initiation, nor were they always found at the center of the sodium channel band. For example, in Figure 6a both the site of lowest threshold and the site of spike initiation occurred in the distal portion of the band. As the stimulating electrode moved further from the soma, the site of spike initiation moved towards the distal edge of the band. The site of spike initiation in pyramidal cells (in response to synaptic input) is also thought to occur in the distal edge of the band, raising the possibility that similar mechanisms of activation may be at work for both synaptic and extracellular activation. In contrast to the offsets observed in the ganglion cell model, the insertion of a non-tapered band into a long axon resulted in both the lowest threshold and the site of initiation being centered in the band (not shown). Presumably, the lower impedance of the soma shunts sub-threshold sodium currents in the proximal axon, raising the spike threshold in those regions. Consequently, the low somatic impedance ‘pushes’ both sites outward while the higher impedance associated with the distal (narrow) end of the band facilitates spike generation.

The site of lowest threshold was at the band midpoint for only the shortest bands (20 μm) that we tested. Because the position of the stimulating electrode was stepped in 2 μm increments, it is possible that a small offset from center in shorter bands might not have been detected.

Nevertheless, our methods would have detected a larger offset, i.e. one that is comparable to the percent offset found in larger bands, suggesting that the offset from center of the low threshold location is larger for longer bands.

4.4. Implications for future modeling studies and for retinal prosthetic development

The ability to improve the quality of vision elicited by retinal prosthetics will depend on many parallel efforts. This study was motivated by the need to understand the mechanisms responsible for neural activity elicited by electric stimulation so that more effective methods

can be developed. . The findings of this study suggest that the response differences to pulsatile electric stimulation across cell types arise, at least in part, from the differences in band properties. One of the important next steps will be to determine whether knowledge of the factors underlying activation can be utilized to selectively target, or avoid individual cell types. For example, use of creative stimulation strategies, i.e. those that use sub-threshold pre-pulses, can reverse the inherent selectivity in axons and allow those axons with lower sensitivity to be preferentially activated[32]. A similar strategy may be useful for the retina as well. While the threshold differences measured physiologically and calculated in our models were in response to short duration pulses, other stimulus waveforms have begun to be evaluated [33; 34]. A more complete understanding of the activation process will enable accurate computational evaluation so that a wide range of stimulus waveforms and parameters do not have to be evaluated physiologically in order to optimize stimulation methods.

4.5. Can the neurons activated during clinical trials be predicted?

Human vision is thought to be mediated primarily by two types of ganglion cells, midget and parasol. The ability to selectively activate either or both of these, especially if the ON and OFF versions of each type were separable, would almost certainly lead to dramatic improvements in the quality of elicited vision. In addition, the ability to selectively activate each type individually would allow psychophysical exploration of the role played by each in generating our visual perception.

A previous study determined that the lowest thresholds occurred when the stimulating electrode was ~13 μm from the soma of primate parasol cells[35]. Because the center of the low threshold region corresponds to the approximate center of the sodium channel band, it can be inferred that the proximal edge of the sodium channel band in primate parasol cells is fairly close to the soma. If so, our findings raise the concern that the close proximity of the band to the soma may be associated with increased thresholds for activation. If parasol cells do in fact have a relatively high threshold, it would necessitate alternative stimulation methods in order for them to be activated. Of course relative threshold predictions cannot be confirmed without knowledge of the sodium channel band length and locations in these (and other) types of ganglion cells. However, once the band properties of all types are known, the relative response to a wide range of stimulation schemes can be predicted via computational model. Schemes that could target individual cell types would likely result in a dramatic improvement in the quality of vision and be an important component of the next generation of stimulation systems.

Acknowledgments

This work was funded in part by the VA Healthcare System (Center for Innovative Visual Rehabilitation), the Dept. of Defense (W81XWH-07-1-0474) and the NIH (1 R01 EY019967-01). We wish to thank Donald Eddington and Daniel Freeman for helpful discussion and for their comments on an early version of the manuscript.

References

1. Stone JL, Barlow WE, Humayun MS, de Juan E Jr, Milam AH. Morphometric analysis of macular photoreceptors and ganglion cells in retinas with retinitis pigmentosa. Arch Ophthalmol. 1992; 110:1634–1639. [PubMed: 1444925]
2. Santos A, Humayun MS, de Juan E Jr, Greenburg RJ, Marsh MJ, Klock IB, Milam AH. Preservation of the inner retina in retinitis pigmentosa. A morphometric analysis. Arch Ophthalmol. 1997; 115:511–515. [PubMed: 9109761]
3. Medeiros NE, Curcio CA. Preservation of ganglion cell layer neurons in age-related macular degeneration. Invest Ophthalmol Vis Sci. 2001; 42:795–803. [PubMed: 11222543]

4. Strettoi E, Pignatelli V, Rossi C, Porciatti V, Falsini B. Remodeling of second-order neurons in the retina of rd/rd mutant mice. Vision Res. 2003; 43:867–877. [PubMed: 12668056]
5. Gargini C, Terzibasi E, Mazzoni F, Strettoi E. Retinal organization in the retinal degeneration 10 (rd10) mutant mouse: a morphological and ERG study. J Comp Neurol. 2007; 500:222–238. [PubMed: 17111372]
6. Marc RE, Jones BW, Watt CB, Strettoi E. Neural remodeling in retinal degeneration. Prog Retin Eye Res. 2003; 22:607–655. [PubMed: 12892644]
7. Humayun MS, de Juan E Jr, Dagnelie G, Greenberg RJ, Propst RH, Phillips DH. Visual perception elicited by electrical stimulation of retina in blind humans. Arch Ophthalmol. 1996; 114:40–46. [PubMed: 8540849]
8. Rizzo JF 3rd, Wyatt J, Loewenstein J, Kelly S, Shire D. Perceptual efficacy of electrical stimulation of human retina with a microelectrode array during short-term surgical trials. Invest Ophthalmol Vis Sci. 2003; 44:5362–5369. [PubMed: 14638739]
9. Weiland JD, Liu W, Humayun MS. Retinal Prothesis. Annu Rev Biomed Eng. 2004
10. Caspi A, Dorn JD, McClure KH, Humayun MS, Greenberg RJ, McMahon MJ. Feasibility study of a retinal prosthesis: spatial vision with a 16-electrode implant. Arch Ophthalmol. 2009; 127:398–401. [PubMed: 19365014]
11. Jensen RJ, Rizzo JF 3rd, Ziv OR, Grumet A, Wyatt J. Thresholds for activation of rabbit retinal ganglion cells with an ultrafine, extracellular microelectrode. Invest Ophthalmol Vis Sci. 2003; 44:3533–3543. [PubMed: 12882804]
12. Tsai D, Morley JW, Suaning GJ, Lovell NH. Direct activation and temporal response properties of rabbit retinal ganglion cells following subretinal stimulation. J Neurophysiol. 2009; 102:2982–2993. [PubMed: 19741103]
13. Schiefer MA, Grill WM. Sites of neuronal excitation by epiretinal electrical stimulation. IEEE Trans Neural Syst Rehabil Eng. 2006; 14:5–13. [PubMed: 16562626]
14. Greenberg RJ, Velte TJ, Humayun MS, Scarlatis GN, de Juan E Jr. A computational model of electrical stimulation of the retinal ganglion cell. IEEE Trans Biomed Eng. 1999; 46:505–514. [PubMed: 10230129]
15. Fried SI, Lasker AC, Desai NJ, Eddington DK, Rizzo JF 3rd. Axonal sodium-channel bands shape the response to electric stimulation in retinal ganglion cells. J Neurophysiol. 2009; 101:1972–1987. [PubMed: 19193771]
16. Jensen RJ, Rizzo JF 3rd. Activation of retinal ganglion cells in wild-type and rd1 mice through electrical stimulation of the retinal neural network. Vision Res. 2008; 48:1562–1568. [PubMed: 18555890]
17. Hines, M. NEURON - a program for simulaiton of nerve equations. Norwell: Kluwer Academic; 1993. p. 127-136.
18. Sheasby BW, Fohlmeister JF. Impulse encoding across the dendritic morphologies of retinal ganglion cells. J Neurophysiol. 1999; 81:1685–1698. [PubMed: 10200204]
19. Carras PL, Coleman PA, Miller RF. Site of action potential initiation in amphibian retinal ganglion cells. J Neurophysiol. 1992; 67:292–304. [PubMed: 1569462]
20. Fohlmeister JF, Coleman PA, Miller RF. Modeling the repetitive firing of retinal ganglion cells. Brain Res. 1990; 510:343–345. [PubMed: 2331606]
21. Fohlmeister JF, Miller RF. Mechanisms by which cell geometry controls repetitive impulse firing in retinal ganglion cells. J Neurophysiol. 1997; 78:1948–1964. [PubMed: 9325363]
22. Jenkins SM, Bennett V. Ankyrin-G coordinates assembly of the spectrin-based membrane skeleton, voltage-gated sodium channels, and L1 CAMs at Purkinje neuron initial segments. J Cell Biol. 2001; 155:739–746. [PubMed: 11724816]
23. Caldwell JH, Schaller KL, Lasher RS, Peles E, Levinson SR. Sodium channel Na(v)1.6 is localized at nodes of ranvier, dendrites, and synapses. Proc Natl Acad Sci U S A. 2000; 97:5616–5620. [PubMed: 10779552]
24. Van Wart A, Trimmer JS, Matthews G. Polarized distribution of ion channels within microdomains of the axon initial segment. J Comp Neurol. 2007; 500:339–352. [PubMed: 17111377]

25. Boiko T, Van Wart A, Caldwell JH, Levinson SR, Trimmer JS, Matthews G. Functional specialization of the axon initial segment by isoform-specific sodium channel targeting. J Neurosci. 2003; 23:2306–2313. [PubMed: 12657689]
26. Kole MH, Ilschner SU, Kampa BM, Williams SR, Ruben PC, Stuart GJ. Action potential generation requires a high sodium channel density in the axon initial segment. Nat Neurosci. 2008; 11:178–186. [PubMed: 18204443]
27. Johns Hopkins; 1998. Published
28. Rush AM, Dib-Hajj SD, Waxman SG. Electrophysiological properties of two axonal sodium channels, Nav1.2 and Nav1.6, expressed in mouse spinal sensory neurones. J Physiol. 2005; 564:803–815. [PubMed: 15760941]
29. Rockhill RL, Daly FJ, MacNeil MA, Brown SP, Masland RH. The diversity of ganglion cells in a mammalian retina. J Neurosci. 2002; 22:3831–3843. [PubMed: 11978858]
30. Zrenner E, Wilke R, Bartz-Schmidt KU, Benav H, Besch D, Gekeler F, Koch J, Porubska K, Sachs H, Wilhelm B. Blind Retinitis Pigmentosa Patients Can Read letters and Recognize the Direction of Fine Stripe Patterns With Subretinal Electronic Implants. Invest Ophthalmol Vis Sci. 2009; 50 Abstract #: 4581.
31. daCruz L, Coley B, Christopher P, Merlini F, Wuyyuru V, Sahel JA, Stanga P, Filley E, Dagnelie G. Patients Blinded by Outer Retinal Dystrophies Are Able to Identify Letters Using the Argus II Retinal Prosthesis System. Invest Ophthalmol Vis Sci. 2010; 51 Abstract #: 2023.
32. Grill WM, Mortimer JT. Inversion of the current-distance relationship by transient depolarization. IEEE Trans Biomed Eng. 1997; 44:1–9. [PubMed: 9214779]
33. Cantrell DR, Troy JB. Extracellular stimulation of mouse retinal ganglion cells with non-rectangular voltage-controlled waveforms. Conf Proc IEEE Eng Med Biol Soc. 2009; 2009:642–645. [PubMed: 19963976]
34. Langille M, Gonzalez-Cueto JA, Sundar S. Analysis of the selective nature of sensory nerve stimulation using different sinusoidal frequencies. Int J Neurosci. 2008; 118:1131–1144. [PubMed: 18576211]
35. Sekirnjak C, Hottowy P, Sher A, Dabrowski W, Litke AM, Chichilnisky EJ. Electrical stimulation of mammalian retinal ganglion cells with multielectrode arrays. J Neurophysiol. 2006; 95:3311–3327. [PubMed: 16436479]

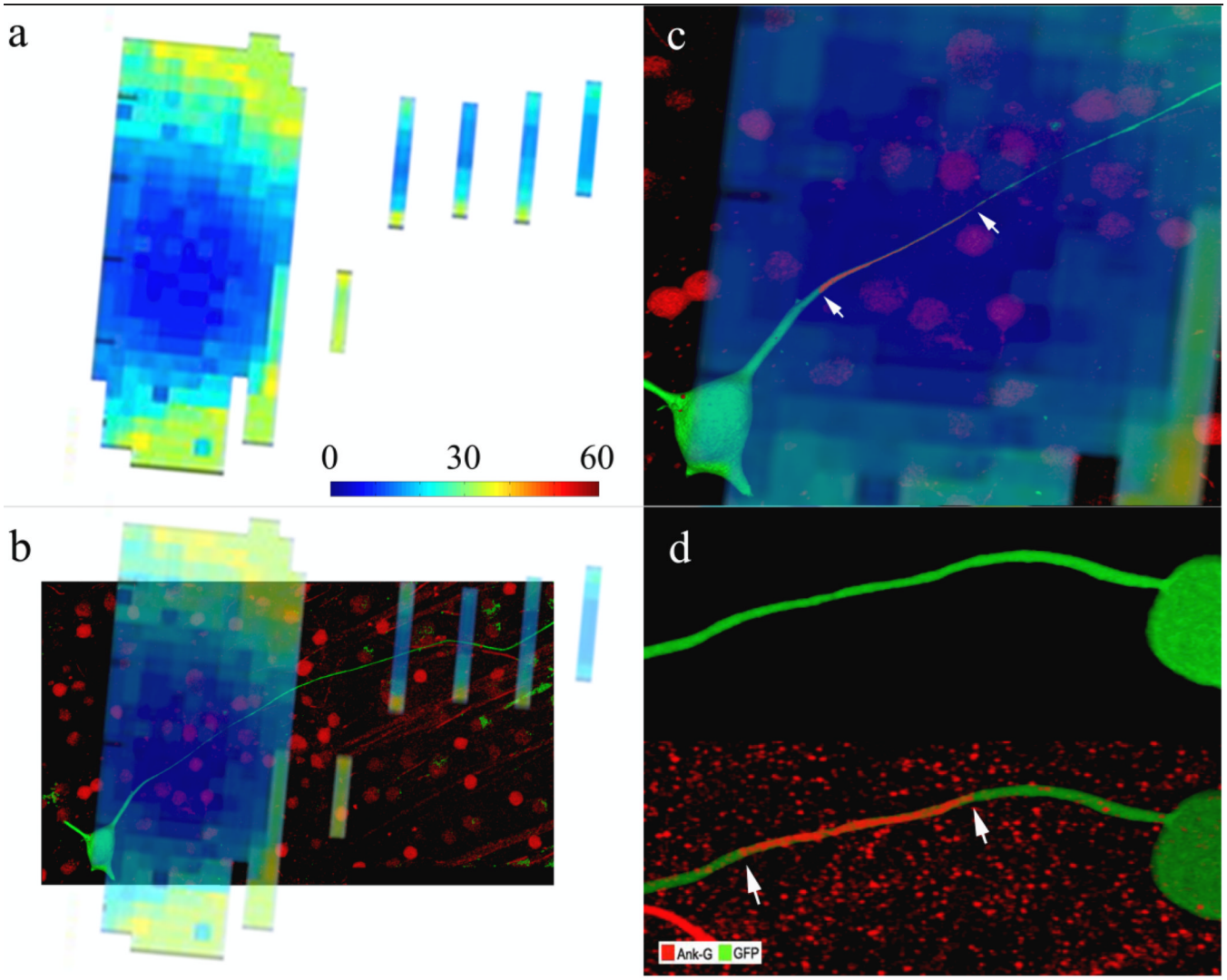

Figure 1. The sodium channel band is the site of maximum sensitivity

(**a**) Threshold map from physiological experiments in which each pixel represents the threshold to a 0.2 ms cathodal pulse at that x-y location. The height of the stimulating electrode was fixed 25 μm above the ganglion cell. Pixel spacing is 10 μm. The colorbar indicates threshold level in μA. (**b**) Overlay of the threshold map with the dye-filled ganglion cell reveals that the region of lowest threshold is aligned with the proximal axon. (**c**) Magnified view of the low threshold region from (b). The ganglion cell has been immunostained for AnkyrinG (red). Arrows indicate the extent of the AnkyrinG when visualized without the overlay. (**d**) Immunostaining for AnkyrinG in a different cell reveals a dense band of sodium channels (arrows) within the proximal axon.

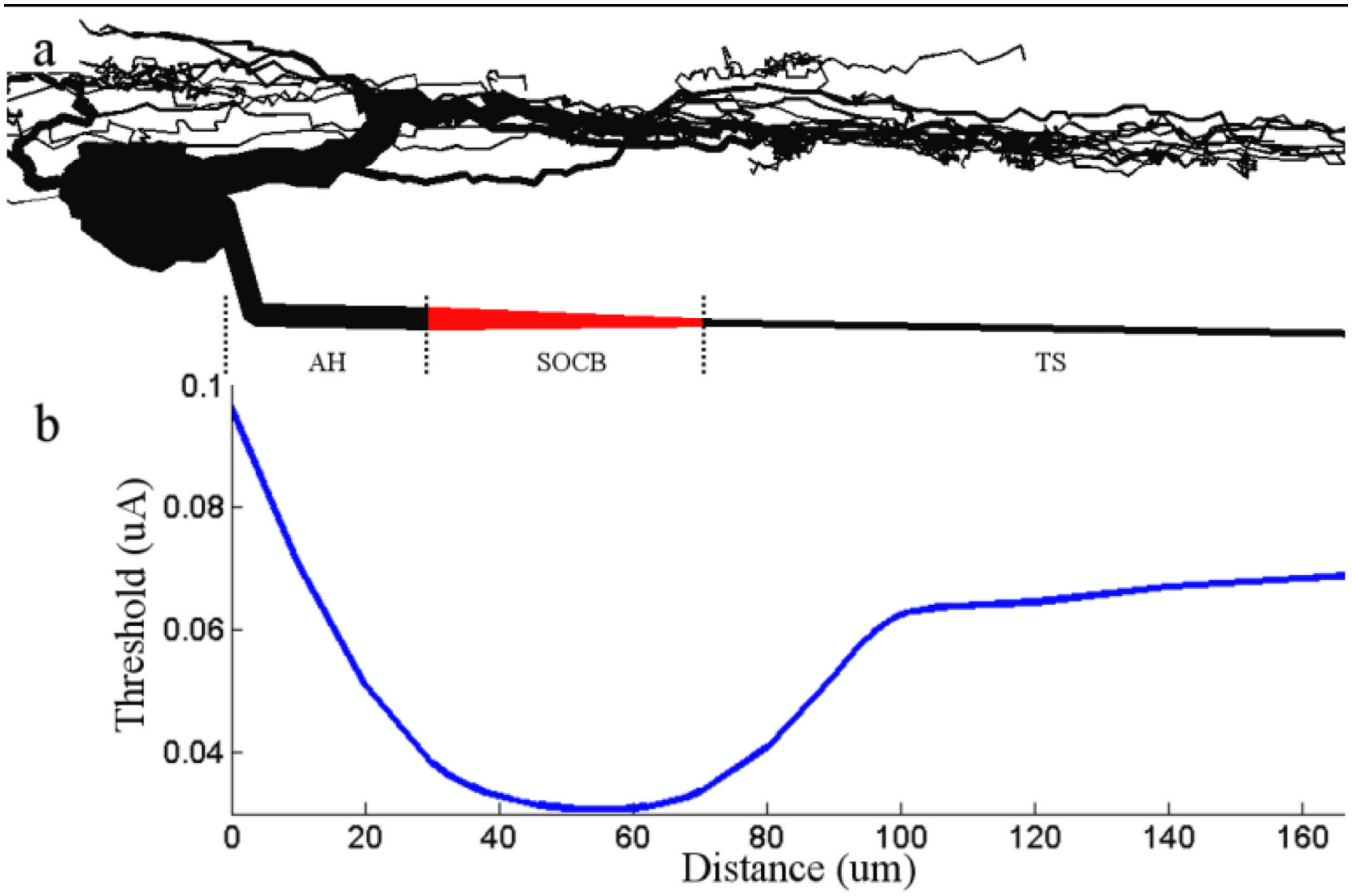

Figure 2. Threshold is lowest at the sodium channel band

(**a**) Schematic of the model ganglion cell. The soma and dendritic field were replicated from Sheasby and Fohlmeister[18]; the morphological and biophysical properties of the axon are described in Table 1. The dense band of voltage gated sodium channels in the proximal axon is indicated in red. (**b**) The threshold for eliciting action potentials with a 0.2 ms cathodal pulse is plotted as a function of electrode location for a 40 μm band that was 30 μm from the soma. The ratio of the band to distal axon sodium channel conductance is 20. (a) and (b) have identical scales and are spatially aligned so that thresholds along the x-axis in (b) can be correlated to the morphological features of (a). AH: axon hillock; SOCB: sodium channel band; TS: thin segment.

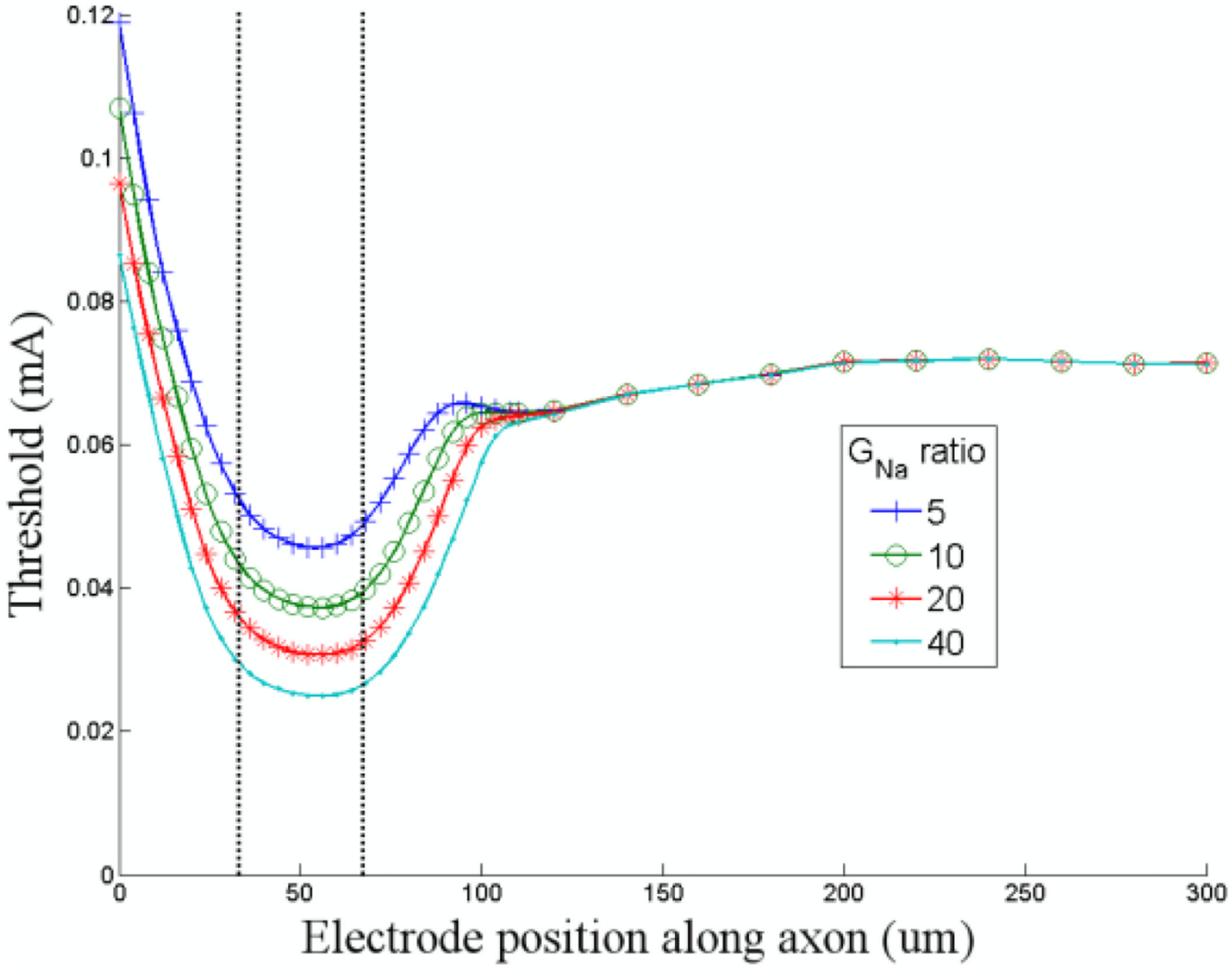

Figure 3. Increased band G_{Na} results in lower activation thresholds

Threshold is plotted as a function of stimulating electrode location for four different levels of sodium channel conductance ($\hat{G}_{Na}$) within the band. The lowest level of $\hat{G}_{Na}$ in the band was a factor of five greater than the $\hat{G}_{Na}$ of the distal axon. The highest level of $\hat{G}_{Na}$ in the band was 40 times the axon $\hat{G}_{Na}$. The vertical lines indicate the edges of the sodium channel band. Zero on the abscissa corresponds to the closest edge of the soma. The minimum thresholds for ratios of 5, 10, 20 and 40 were 0.046, 0.037, 0.031 and 0.025 mA (respectively).

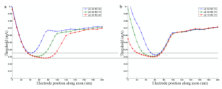

Figure 4. Band length and location influence threshold

(**a**) Threshold as a function of stimulating electrode position for a model cell ($\hat{G}_{Na}$ ratio of 20) tested with three different band lengths. The left edge of the band was fixed at a distance of 30 μm from the soma for all simulations. The lower and upper horizontal lines indicate the minimum threshold for the longest band (60 μm) and the shortest band (20 μm) respectively (**b**) Similar to (a) except the right edge of the band was now fixed at a distance of 70 μm for all simulations. The horizontal lines extended from (a) allow comparisons of threshold between the plots. LE: distance from the soma to the left (proximal) edge of the band (in μm); RE: distance from the soma to the right (distal) edge of the band.

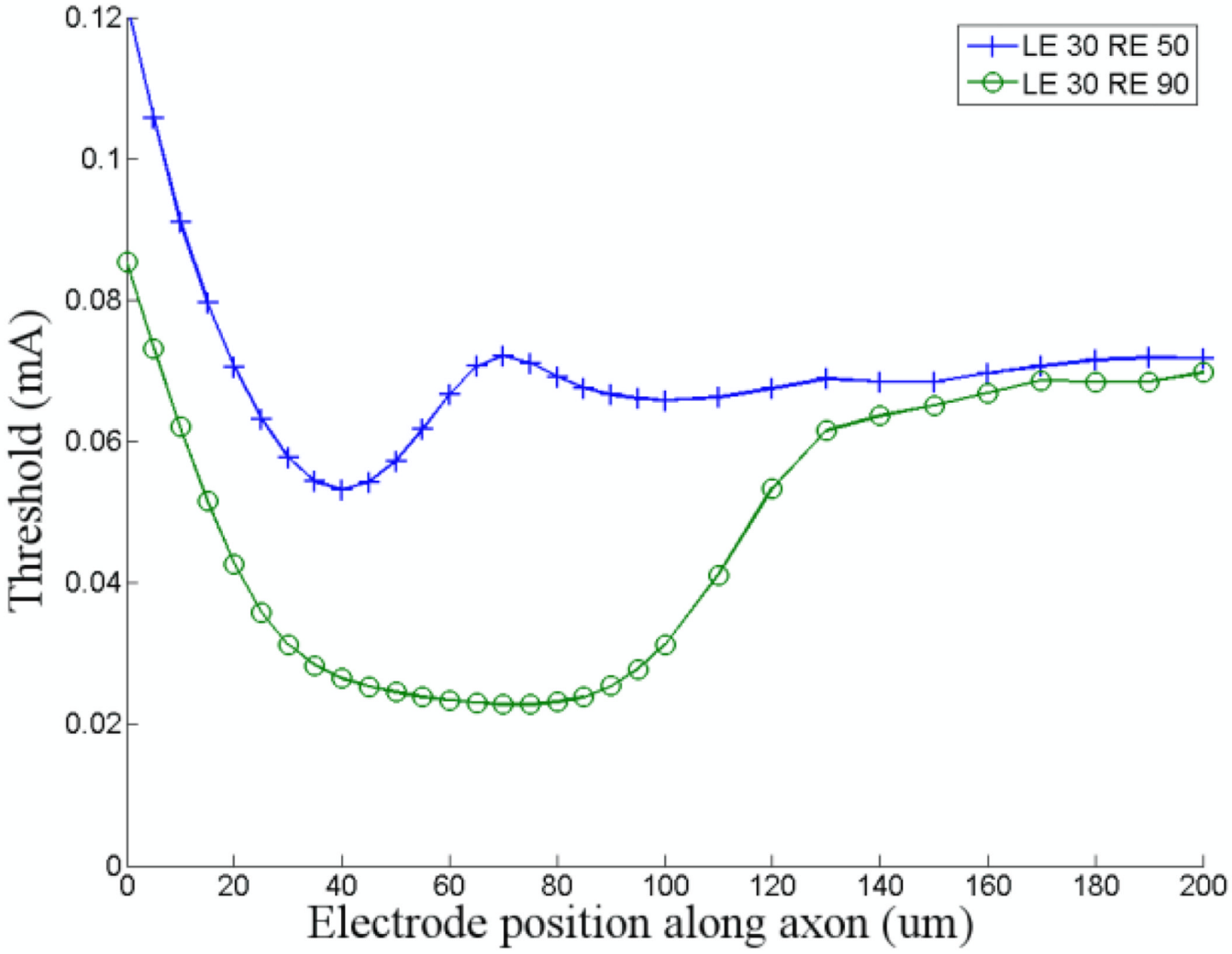

Figure 5. Estimating the range of thresholds

Thresholds in the high- and low-threshold models (see text) are plotted as a function of the position of the stimulating electrode (vertical tick marks and circles, respectively). LE: distance from the soma to the left (proximal) edge of the band (in μm); RE: distance from the soma to the right edge of the band.

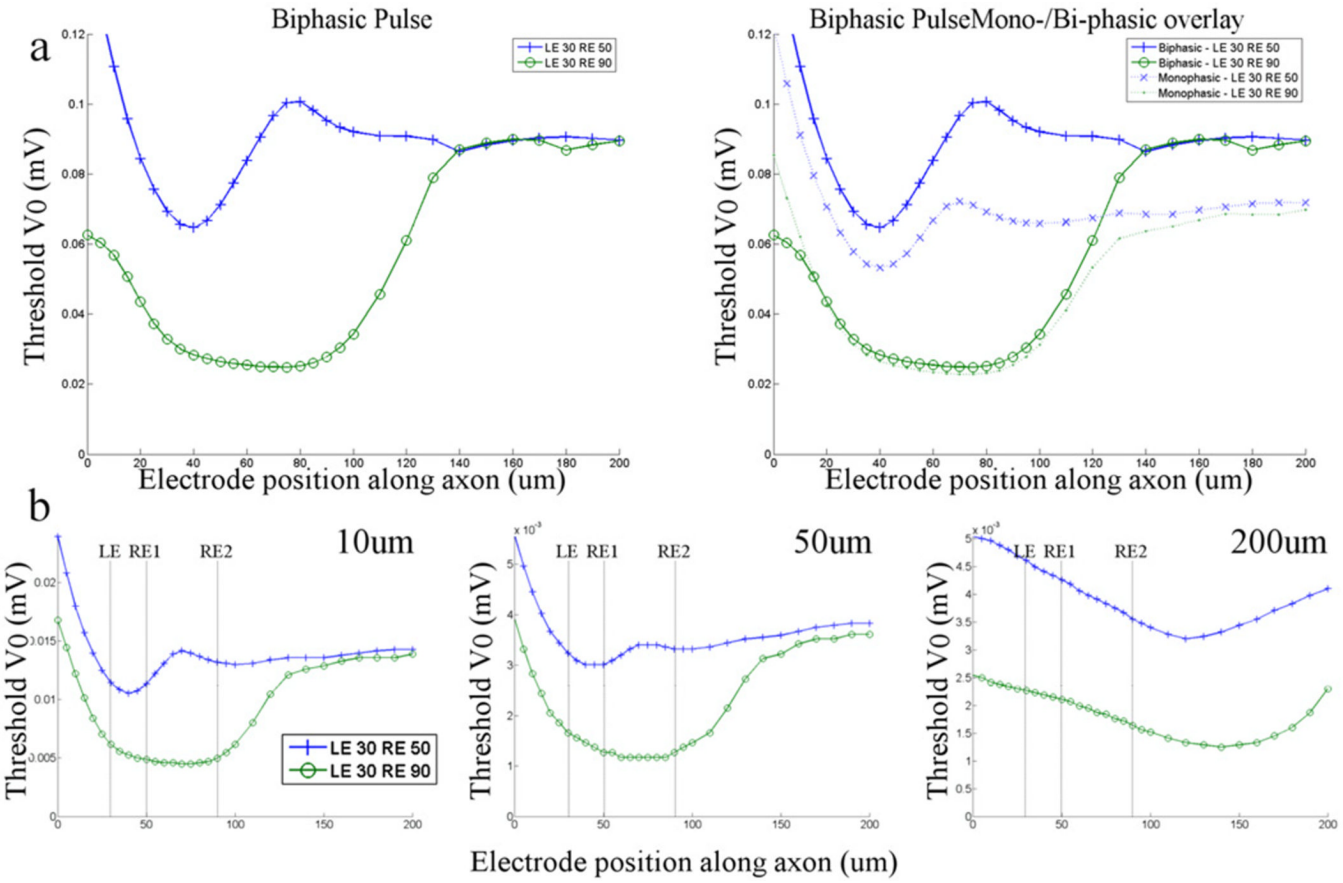

Figure 6. Stimulus waveform and electrode size influence the range of thresholds

(a, left) Thresholds in the high- and low-threshold models (see text) are plotted as a function of the position of the stimulating electrode (vertical tick marks and circles, respectively) for biphasic waveforms. (**a, right**) Overlay of the biphasic response and the cathodal response. LE: distance from the soma to the left (proximal) edge of the band (in μm); RE: distance from the soma to the right edge of the band. (**b**) Thresholds are plotted in response to stimulation from disk electrodes in the high- and low-threshold models. The diameter of the disk electrode was 10, 50 and 200 um (left, middle and right panels). RE1 indicates the right edge of the band for the high-threshold model; RE2 is the right edge for the low threshold model.

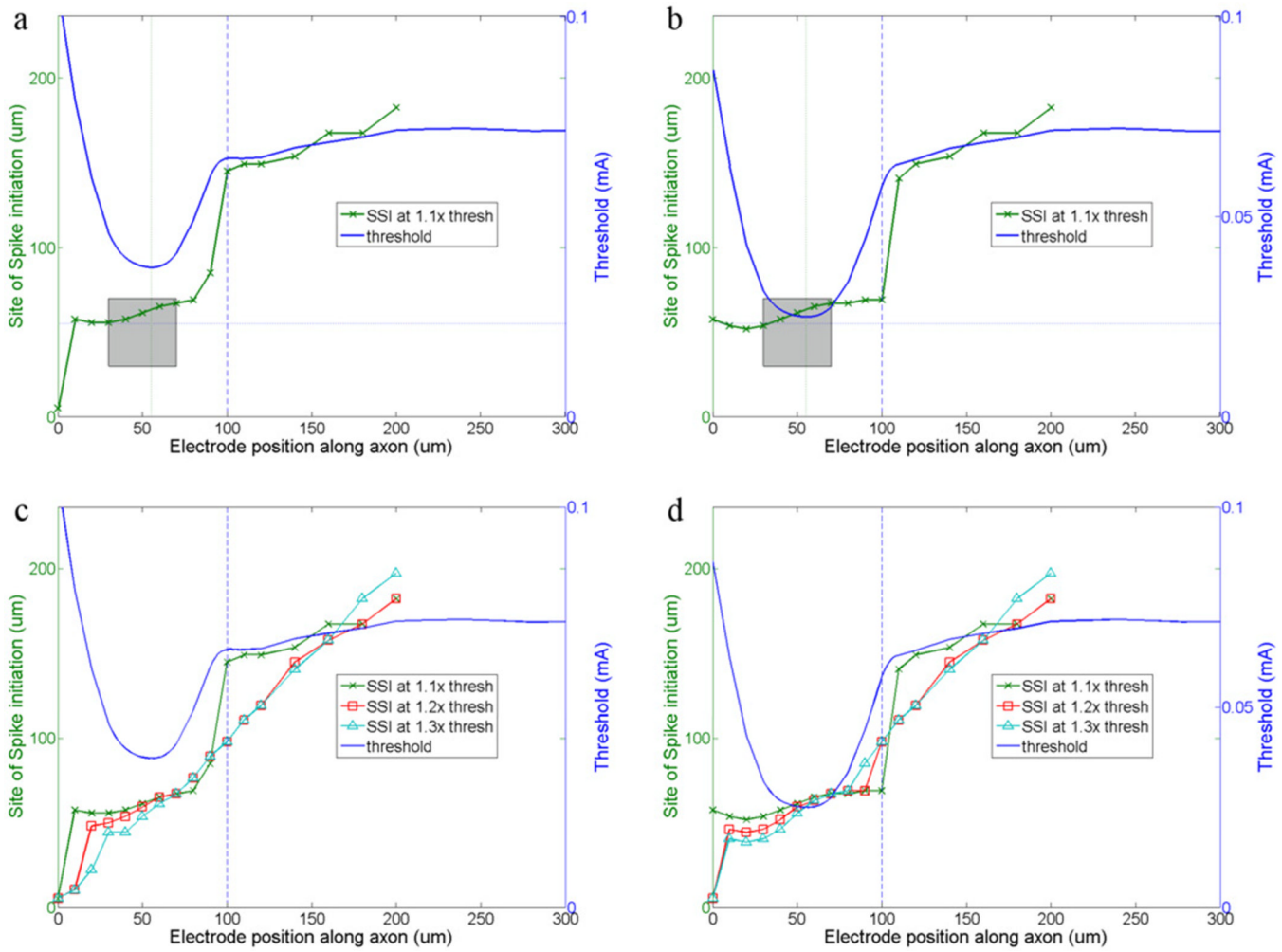

Figure 7. The site of spike initiation is influenced by electrode position and band properties

(**a**) Threshold and site of spike initiation (SSI) are both plotted as a function of stimulating electrode position. The amplitude of the stimulus pulse was fixed at 1.1× threshold and the band to soma G_{Na} ratio was fixed at 5. The vertical line indicates a distance of 100um from the soma and is used to compare results in (b). The shaded box marks the edges of the band for both axes. The thin vertical line indicates the location of the stimulating electrode for which threshold was minimum; the thin horizontal line indicates the same location. (**b**) Similar to (a) except the G_{Na} ratio is 40. (**c, d**) Similar to (a) and (b) respectively, except additional runs were made with the stimulus amplitude increased to both 1.2× and 1.3× threshold. In all plots the vertical lines at 30 and 70 μm indicate the extent of the band relative to the position of the stimulating electrode (x-axis) and horizontal lines (at 30 and 70 μm (right y-axis), indicate the extent of the band relative to the site of spike initiation. In all panels, the thin section extends from 90–160 μm.

Table 1

Properties of the sodium channel band

	Axon				Soma	Dendrites
	AH	SOCB	TS	DA		
Diameter (μm) (proximal end)	3	3	0.8	1		
Diameter (μm) (distal end)	3	0.8	0.8	1		
Length (μm)	41	40	90	5300		
$\hat{G}_{Na}$ (E_{Na}=+35mV)	70	350–2800	100	70	80	25
$\hat{G}_{K,DR}$ (E_K=−75mV)	18	9–72	18	18	18	12
$\hat{G}_A$ (E_K=−75mV)		54	54		54	36
$\hat{G}_{Ca}$ (E_{Ca}=132mV)		1.5			1.5	2
$\hat{G}_{K,Ca}$	0.065	0.065	0.065	0.065	0.065	0.001
$\hat{G}_l$	0.005	0.005	0.005	0.005	0.005	0.005
Conductances are in pS/cm^2						
Number of segments	99	21	21	354	21	536

Table 2

Ion Channel Kinetics

Ion	Channel	State Variable	α	β
Na	Fast sodium	m	$\frac{-0.6*(V+30)}{e^{-0.1*(v+30)}-1}$	$\frac{20}{e^{\frac{v+55}{18}}}$
		h	$\frac{0.4}{e^{\frac{v+50}{20}}}$	$\frac{6}{1+e^{-0.1*(v+20)}}$
K	Delayed rectifier	n	$\frac{-0.02*(v+40)}{(e^{-0.1*(v+40)})-1}$	$\frac{0.4}{e^{\frac{v+50}{80}}}$
	A-type	a	$\frac{-0.006*(v+90)}{(e^{-0.1*(v+90)})-1}$	$\frac{0.1}{e^{\frac{v+30}{10}}}$
		h_A	$\frac{0.04}{e^{\frac{v+70}{20}}}$	$\frac{-0.6}{e^{-0.1*(v+40)}+1}$
	Calcium activated	$I_{K,Ca}=\widehat{G}_{K,Ca}\left(\frac{[Ca]_i/0.001}{1+[Ca]_i/0.001}\right)(v-e_k)$		
Ca	Ca	c	$\frac{-0.3*(v+13)}{(e^{-0.1*(v+13)})-1}$	$\frac{10}{e^{\frac{v+38}{18}}}$